

Optimal Prediction of Tessarine Signals from Multi-sensor Uncertain Observations under \mathbb{T}_k -Properness Conditions

José Domingo Jiménez-López^a, Rosa María Fernández-Alcalá^b, Jesús Navarro-Moreno^c
and Juan Carlos Ruiz-Molina^d

Department of Statistics and Operations Research, University of Jaén, Paraje Las Lagunillas s/n, 23071 Jaén, Spain

Keywords: Multisensor Systems, Optimal Prediction, Tessarine Signal Processing, \mathbb{T}_k -Properness Conditions, Uncertain Observations.

Abstract: In this paper, the optimal one-stage prediction problem of tessarine signals from multi-sensor uncertain observations is approached. At each instant of time, there exists a non-null probability that the observation tessarine component coming from each sensor, contains the corresponding signal component, or only noise. To model the uncertainty, multiplicative noises modeled by Bernoulli random variables are included in the observation equations. Under correlation hypotheses between the signal and observation additive noises, a recursive algorithm to calculate the optimal least-squares linear predictor of the signal and its mean-squared error is proposed, derived by using an innovation approach. The theoretical results are illustrated by means of a numerical simulation example, in which the performance of the proposed estimator is evaluated under different uncertainty probabilities.


1 INTRODUCTION


Traditionally, the real and complex domains have constituted the framework to model random signals in dynamical systems. However, in the last two decades, there has been an increasing interest in the scientific community to study higher-dimensional spaces, due to the fact that they are more appropriate to model a great number of physical phenomena. As an example, hypercomplex signals are used to model biomedical phenomena (Abbasi-Kesbi and Nikfarjam, 2018; Ajudaroski et al., 2022), avionics, as unmanned aerial vehicles (Zheng et al., 2020; Qu and Yi, 2022), neural networks (Bayro-Corrochano et al., 2021; Wei et al., 2022), acoustic applications (Ortolani et al., 2016; Celsi et al., 2020), communication (Grakhova et al., 2019; Ahmad et al., 2021), image processing (Augereau and Carré, 2017; Yang et al., 2022), etc.


Recently, in real signal processing, estimation problems have been approached from observations provided by multiple sensors. The fact that the signal is estimated from multisensor observations, yields


better estimates than those traditionally obtained by a single sensor, since more observations are available, and also it is possible to avoid the negative effect in the estimation caused by observations from faulty sensors. In the real domain, there exists a wide-ranging literature on signal processing from multisensor observations affected by different uncertainties, that frequently occur in the transmission problems. For example, assuming missing or intermittent measurements, the estimation problem has been solved in the real field by using the centralized fusion method (Liu et al., 2017) and the distributed fusion procedure (Lin and Sun, 2016). Another common situation consists of considering that the observations may be updated or delayed at each instant of time (Linares-Pérez et al., 2009; Liang et al., 2011). Both uncertainties can be also simultaneously studied (Zhang et al., 2021), or even include multiple packet dropouts, in which case the last observation successfully transmitted is considered if the real observation is not available (Ma and Sun, 2013).

So, the need to extend the obtained results on the real signal estimation problems to the hypercomplex domains arises. However, this generalization is not an immediate extension from the real vectorial case, due to the fact that the hypercomplex algebras lose important properties of the algebraic operations in the

^a  <https://orcid.org/0000-0003-1263-5508>

^b  <https://orcid.org/0000-0002-3329-6624>

^c  <https://orcid.org/0000-0002-8417-8505>

^d  <https://orcid.org/0000-0002-3128-8030>

real field. Moreover, under certain properties of the processes involved in the system model, a reduction in the dimension of the model is obtained, fact that it can not be considered in the real field. Most of the estimation problems in the hypercomplex domains have been studied in the quaternion space, due to the fact that it has a Hilbert space structure, although the product is not commutative. In the quaternion domain, the widely linear (WL) estimation problem, that is, that means to consider the signal and its three involutions, has been solved under different uncertainty hypotheses (Jiménez-López et al., 2017; Fernández-Alcalá et al., 2020). Assuming \mathbb{C}^n -property conditions, the processing is called semi-widely linear (SWL) one, and it considers the signal and the involution over the pure unit quaternion (Navarro-Moreno et al., 2019).

The signal estimation problems in the tessarine domain have been less studied since it is not a Hilbert space. Recently, a metric has been defined in the tessarine domain that satisfies the necessary properties to guarantee the existence and uniqueness of the least-squares linear estimator (Navarro-Moreno et al., 2020). Moreover, from analogy with the quaternion domain, \mathbb{T}_1 and \mathbb{T}_2 -properness conditions have been defined in the tessarine domain, getting so a reduction in the dimension of the model (Navarro-Moreno et al., 2020; Navarro-Moreno and Ruiz-Molina, 2021; Fernández-Alcalá et al., 2021).

In this paper, the least-squares linear one-stage prediction problem is approached by considering a state-space model with uncertain observations provided by multiple sensors. Under correlation hypotheses on the additive noises and \mathbb{T}_k -properness conditions, a recursive prediction algorithm is proposed. A numerical simulation example illustrates the theoretical results obtained.

2 MODEL FORMULATION

In this section, the tessarine state-space model is presented by means of the signal and multi-sensor observation equations. Notation \mathbb{R} and \mathbb{T} will be used to the set of real numbers and tessarine field, respectively. Moreover, unless otherwise stated, all the random variables are assumed to have zero-mean.

Let us consider a n -dimensional tessarine random signal vector $\mathbf{x}(t) \in \mathbb{T}^n$, which is given as follows

$$\mathbf{x}(t) = \mathbf{x}_r(t) + \eta \mathbf{x}_\eta(t) + \eta' \mathbf{x}_{\eta'}(t) + \eta'' \mathbf{x}_{\eta''}(t), \quad (1)$$

where $\mathbf{x}_v(t) \in \mathbb{R}^n$, for $v = r, \eta, \eta', \eta''$, are n -dimensional real random signal vector and $\{\eta, \eta', \eta''\}$ denote the imaginary units satisfying the following

identities:

$$\begin{aligned} \eta\eta' &= \eta'', & \eta'\eta'' &= \eta, & \eta''\eta &= -\eta', \\ \eta^2 &= -\eta'^2 = \eta''^2 = -1. \end{aligned}$$

Let us assume the following state equation for $\mathbf{x}(t)$:

$$\begin{aligned} \mathbf{x}(t+1) &= \mathbf{F}_1(t)\mathbf{x}(t) + \mathbf{F}_2(t)\mathbf{x}^*(t) + \mathbf{F}_3(t)\mathbf{x}^\eta(t) \\ &+ \mathbf{F}_4(t)\mathbf{x}^{\eta''}(t) + \mathbf{u}(t), \quad t \geq 0, \end{aligned} \quad (2)$$

where $\mathbf{F}_i(t) \in \mathbb{T}^{n \times n}$, for $i = 1, \dots, 4$, are tessarine deterministic matrices of dimension $n \times n$, $\mathbf{x}^v(t)$, for $v = *, \eta, \eta''$, are the corresponding conjugations of the tessarine signal in (1), defined as follows

$$\begin{aligned} \mathbf{x}^*(t) &= \mathbf{x}_r(t) - \eta \mathbf{x}_\eta(t) + \eta' \mathbf{x}_{\eta'}(t) - \eta'' \mathbf{x}_{\eta''}(t), \\ \mathbf{x}^\eta(t) &= \mathbf{x}_r(t) + \eta \mathbf{x}_\eta(t) - \eta' \mathbf{x}_{\eta'}(t) - \eta'' \mathbf{x}_{\eta''}(t), \\ \mathbf{x}^{\eta''}(t) &= \mathbf{x}_r(t) - \eta \mathbf{x}_\eta(t) - \eta' \mathbf{x}_{\eta'}(t) + \eta'' \mathbf{x}_{\eta''}(t), \end{aligned}$$

and $\mathbf{u}(t) \in \mathbb{T}^n$ is a tessarine white noise with *pseudo* variance matrix $\mathbf{Q}(t)$.

Consider that the signal $\mathbf{x}(t)$ is estimated from the observations provided by m sensors, denoted by $\mathbf{y}^{(i)}(t) \in \mathbb{T}^n$, for $i = 1, \dots, m$, satisfying the following observation equation:

$$\begin{aligned} \mathbf{y}^{(i)}(t) &= \gamma_r^{(i)}(t) \circ \mathbf{x}_r(t) + \eta \gamma_\eta^{(i)}(t) \circ \mathbf{x}_\eta(t) \\ &+ \eta' \gamma_{\eta'}^{(i)}(t) \circ \mathbf{x}_{\eta'}(t) + \eta'' \gamma_{\eta''}^{(i)}(t) \circ \mathbf{x}_{\eta''}(t) \\ &+ \mathbf{v}^{(i)}(t), \quad t \geq 1, \end{aligned} \quad (3)$$

where \circ denotes the Hadamard product, and $\mathbf{v}^{(i)}(t) \in \mathbb{T}^n$ is a tessarine white noise with *pseudo* variance matrix $\mathbf{R}^{(i)}(t)$. Moreover, for each sensor $i = 1, \dots, m$, and $v = r, \eta, \eta', \eta''$, $\gamma_v^{(i)}(t)$ is a n -dimensional vector whose components, $\gamma_{j,v}^{(i)}(t)$, are Bernoulli random variables with known parameters $p_{j,v}^{(i)}(t)$. So, if $\gamma_{v,j}^{(i)}(t) = 1$, then the component $y_{j,v}^{(i)}(t)$ contains signal and noise, and in contrast, if it takes the value 0, then the corresponding observation component contains only noise.

Let us assume that for each sensor $i = 1, \dots, m$, and $v = r, \eta, \eta', \eta''$, the Bernoulli random variables in $\gamma_v^{(i)}(t)$ are independent of those in $\gamma_v^{(i)}(s)$, for $s \neq t$. Moreover, $\mathbf{v}^{(i)}(t)$ is independent of $\mathbf{v}^{(j)}(t)$ for $i, j = 1, \dots, m$, with $i \neq j$. The additive noises are correlated, $E[\mathbf{u}(t)\mathbf{v}^{(i)\mathbb{H}}(t)] = \mathbf{S}^{(i)}(t)$ (where \mathbb{H} denotes the Hermitian operator), and \mathbf{P}_0 denotes the *pseudo* variance matrix of the signal at the initial state. Finally, let us consider that $\mathbf{x}(0)$ and the noises $\{\mathbf{u}(t); t \geq 0\}$, $\{\mathbf{v}^{(i)}(t); t \geq 1\}$ and $\{\gamma_v^{(i)}(t); t \geq 1\}$, for $v = r, \eta, \eta', \eta''$, $i = 1, \dots, m$, are mutually independent.

From equations (2) and (3), the following augmented state-space model can be obtained

$$\begin{aligned} \bar{\mathbf{x}}(t+1) &= \bar{\Phi}(t)\bar{\mathbf{x}}(t) + \bar{\mathbf{u}}(t), \quad t \geq 0, \\ \bar{\mathbf{y}}^{(i)}(t) &= \mathcal{D}^{(i)}(t)\bar{\mathbf{x}}(t) + \bar{\mathbf{v}}^{(i)}(t), \quad t \geq 1, \end{aligned} \quad (4)$$

where $\bar{\mathbf{a}}(t) = \left[\mathbf{a}^\top(t), \mathbf{a}^{*\top}(t), \mathbf{a}^{\eta^\top}(t), \mathbf{a}^{\eta''\top}(t) \right]^\top$, for $\mathbf{a} = \mathbf{x}, \mathbf{u}, \mathbf{y}^{(i)}, \mathbf{v}^{(i)}$, where \top denotes the transpose operator,

$$\bar{\Phi}(t) = \begin{bmatrix} \mathbf{F}_1(t) & \mathbf{F}_2(t) & \mathbf{F}_3(t) & \mathbf{F}_4(t) \\ \mathbf{F}_2^*(t) & \mathbf{F}_1^*(t) & \mathbf{F}_4^*(t) & \mathbf{F}_3^*(t) \\ \mathbf{F}_3^\eta(t) & \mathbf{F}_4^\eta(t) & \mathbf{F}_1^\eta(t) & \mathbf{F}_2^\eta(t) \\ \mathbf{F}_4^{\eta''}(t) & \mathbf{F}_3^{\eta''}(t) & \mathbf{F}_2^{\eta''}(t) & \mathbf{F}_1^{\eta''}(t) \end{bmatrix},$$

$$\mathcal{D}^{\gamma^{(i)}}(t) = \mathcal{T}_n \text{diag}(\gamma^{(i)r}(t)) \mathcal{T}_n^H,$$

with $\gamma^{(i)r}(t) = \left[\gamma_r^{(i)\top}(t), \gamma_\eta^{(i)\top}(t), \gamma_{\eta'}^{(i)\top}(t), \gamma_{\eta''}^{(i)\top}(t) \right]^\top$, $\text{diag}(\gamma^{(i)r}(t))$ denotes a diagonal matrix with the elements $\gamma^{(i)r}(t)$ on the main diagonal, and $\mathcal{T}_n = \frac{1}{2} \mathcal{A} \otimes \mathbf{I}_n$, with

$$\mathcal{A} = \begin{bmatrix} 1 & \eta & \eta' & \eta'' \\ 1 & -\eta & \eta' & -\eta'' \\ 1 & \eta & -\eta' & -\eta'' \\ 1 & -\eta & -\eta' & \eta'' \end{bmatrix},$$

and \mathbf{I}_n the identity matrix of dimension n .

The *pseudo* variance matrices of the additive noises $\bar{\mathbf{u}}(t)$ and $\bar{\mathbf{v}}^{(i)}(t)$ in (4) are denoted by $\bar{\mathbf{Q}}(t)$ and $\bar{\mathbf{R}}^{(i)}(t)$, respectively. Moreover, $E \left[\bar{\mathbf{u}}(t) \bar{\mathbf{v}}^{(i)H}(s) \right] = \bar{\mathbf{S}}^{(i)}(t) \delta_{t,s}$, where δ denotes the Kronecker delta function, and $E \left[\bar{\mathbf{x}}(0) \bar{\mathbf{x}}^H(0) \right] = \bar{\mathbf{P}}_0$.

2.1 \mathbb{T}_k -Properness Conditions

The \mathbb{T}_k -properness concept, for $k = 1, 2$, has been recently defined (Navarro-Moreno et al., 2020; Navarro-Moreno and Ruiz-Molina, 2021), and it is related with the fact that some of the *pseudo* correlation functions of the signal with its conjugations vanish. This property reduces the dimension of the augmented state model and, hence, the computational burden necessary to carry out the estimations decreases.

The *pseudo autocorrelation function* of the random signal $\mathbf{x}(t) \in \mathbb{T}^n$ is defined as $\Gamma_{\mathbf{x}}(t, s) = E \left[\mathbf{x}(t) \mathbf{x}^H(s) \right]$, $\forall t, s \in \mathbb{Z}$ (\mathbb{Z} denotes the set of integer), and the *pseudo cross correlation function* of the random signals $\mathbf{x}(t) \in \mathbb{T}^{n_1}$ and $\mathbf{y}(t) \in \mathbb{T}^{n_2}$ is defined as $\Gamma_{\mathbf{xy}}(t, s) = E \left[\mathbf{x}(t) \mathbf{y}^H(s) \right]$, $\forall t, s \in \mathbb{Z}$.

A random signal $\mathbf{x}(t) \in \mathbb{T}^n$ is said to be:

- \mathbb{T}_1 -proper, if, and only if,

$$\Gamma_{\mathbf{xx}^*}(t, s) = \Gamma_{\mathbf{xx}^\eta}(t, s) = \Gamma_{\mathbf{xx}^{\eta''}}(t, s) = \mathbf{0},$$

- \mathbb{T}_2 -proper, if, and only if,

$$\Gamma_{\mathbf{xx}^\eta}(t, s) = \Gamma_{\mathbf{xx}^{\eta''}}(t, s) = \mathbf{0},$$

for all $t, s \in \mathbb{Z}$. Similarly, two random signals $\mathbf{x}(t) \in \mathbb{T}^{n_1}$ and $\mathbf{y}(t) \in \mathbb{T}^{n_2}$ are:

- cross \mathbb{T}_1 -proper, if, and only if,

$$\Gamma_{\mathbf{xy}^*}(t, s) = \Gamma_{\mathbf{xy}^\eta}(t, s) = \Gamma_{\mathbf{xy}^{\eta''}}(t, s) = \mathbf{0},$$

- cross \mathbb{T}_2 -proper, if, and only if,

$$\Gamma_{\mathbf{xy}^\eta}(t, s) = \Gamma_{\mathbf{xy}^{\eta''}}(t, s) = \mathbf{0},$$

for all $t, s \in \mathbb{Z}$. Finally, $\mathbf{x}(t)$ and $\mathbf{y}(t)$ are jointly \mathbb{T}_1 -proper (respectively, jointly \mathbb{T}_2 -proper) if, and only if, they are \mathbb{T}_1 -proper (respectively, \mathbb{T}_2 -proper) and cross \mathbb{T}_1 -proper (respectively, cross \mathbb{T}_2 -proper).

For the model described in equation (4), the following \mathbb{T}_k -properness conditions can be established:

1. If $\mathbf{x}(0)$ and $\mathbf{u}(t)$ are \mathbb{T}_1 -proper, and $\bar{\Phi}(t)$ is a block diagonal matrix of the form

$$\bar{\Phi}(t) = \text{diag} \left(\mathbf{F}_1(t), \mathbf{F}_1^*(t), \mathbf{F}_1^\eta(t), \mathbf{F}_1^{\eta''}(t) \right),$$

then $\mathbf{x}(t)$ is \mathbb{T}_1 -proper. If additionally $p_{j,v}^{(i)}(t) \equiv p_j^{(i)}(t)$, for all $i = 1, \dots, m, j = 1, \dots, n, v = r, \eta, \eta', \eta'', t \in \mathbb{Z}$, $\mathbf{v}^{(i)}(t)$ is \mathbb{T}_1 -proper, and $\mathbf{u}(t)$ and $\mathbf{v}^{(i)}(t)$ are cross \mathbb{T}_1 -proper, then $\mathbf{x}(t)$ and $\mathbf{y}^{(i)}(t)$ are jointly \mathbb{T}_1 -proper. Under these conditions,

$$\Pi^{(i)}(t) = E \left[\mathcal{D}^{\gamma^{(i)}}(t) \right] = \mathbf{I}_4 \otimes \Pi_1^{(i)}(t), \quad i = 1, \dots, m,$$

with

$$\Pi_1^{(i)}(t) = \text{diag} \left(p_{1,r}^{(i)}(t), \dots, p_{n,r}^{(i)}(t) \right), \quad i = 1, \dots, m. \quad (5)$$

2. Analogously, if $\mathbf{x}(0)$ and $\mathbf{u}(t)$ are \mathbb{T}_2 -proper, and $\bar{\Phi}(t)$ is a block diagonal matrix of the form

$$\bar{\Phi}(t) = \text{diag} \left(\Phi_2(t), \Phi_2^\eta(t) \right),$$

with

$$\Phi_2(t) = \begin{bmatrix} \mathbf{F}_1(t) & \mathbf{F}_2(t) \\ \mathbf{F}_2^*(t) & \mathbf{F}_1^*(t) \end{bmatrix}, \quad (6)$$

then $\mathbf{x}(t)$ is \mathbb{T}_2 -proper. If additionally $p_{j,r}^{(i)}(t) = p_{j,\eta}^{(i)}(t)$ and $p_{j,\eta'}^{(i)}(t) = p_{j,\eta''}^{(i)}(t)$, $i = 1, \dots, m, j = 1, \dots, n, t \in \mathbb{Z}$, $\mathbf{v}^{(i)}(t)$ is \mathbb{T}_2 -proper, and $\mathbf{u}(t)$ and $\mathbf{v}^{(i)}(t)$ are cross \mathbb{T}_2 -proper, then $\mathbf{x}(t)$ and $\mathbf{y}^{(i)}(t)$ are jointly \mathbb{T}_2 -proper. In that case,

$$\Pi^{(i)}(t) = \text{diag} \left(\Pi_2^{(i)}(t), \Pi_2^{(i)}(t) \right), \quad i = 1, \dots, m,$$

with

$$\Pi_2^{(i)}(t) = \frac{1}{2} \begin{bmatrix} \Pi_+^{(i)}(t) & \Pi_-^{(i)}(t) \\ \Pi_-^{(i)}(t) & \Pi_+^{(i)}(t) \end{bmatrix}, \quad i = 1, \dots, m, \quad (7)$$

and

$$\begin{aligned}\Pi_+^{(i)}(t) &= \text{diag} \left(p_{1,r}^{(i)}(t) + p_{1,\eta'}^{(i)}(t), \dots \right. \\ &\quad \left. \dots, p_{n,r}^{(i)}(t) + p_{n,\eta'}^{(i)}(t) \right), \\ \Pi_-^{(i)}(t) &= \text{diag} \left(p_{1,r}^{(i)}(t) - p_{1,\eta'}^{(i)}(t), \dots \right. \\ &\quad \left. \dots, p_{n,r}^{(i)}(t) - p_{n,\eta'}^{(i)}(t) \right),\end{aligned}$$

for $i = 1, \dots, m$.

2.2 \mathbb{T}_k -Proper System Model

Under \mathbb{T}_k -properness conditions, a reduction in the dimension of the system model described in (4) is obtained. Next the new situations are described.

- In the \mathbb{T}_1 -proper scenario. The processes $\bar{\mathbf{x}}(t)$, $\bar{\mathbf{u}}(t)$, $\bar{\mathbf{y}}^{(i)}(t)$, $\bar{\mathbf{v}}^{(i)}(t)$ and $\bar{\Phi}(t)$, are substituted by $\mathbf{x}_1(t) \triangleq \mathbf{x}(t)$, $\mathbf{u}_1(t) \triangleq \mathbf{u}(t)$, $\mathbf{y}_1^{(i)}(t) \triangleq \mathbf{y}^{(i)}(t)$, $\mathbf{v}_1^{(i)}(t) \triangleq \mathbf{v}^{(i)}(t)$ and $\Phi_1(t) \triangleq \mathbf{F}_1(t)$. The *pseudo* variance and cross-covariance matrices of the noises are given by $\mathbf{Q}_1(t) = \mathbf{Q}(t)$, $\mathbf{R}_1^{(i)}(t) = \mathbf{R}^{(i)}(t)$ and $\mathbf{S}_1^{(i)}(t) = \mathbf{S}^{(i)}(t)$. The observation equation in (4) is now expressed as follows

$$\mathbf{y}_1^{(i)}(t) = \mathcal{D}_1^{\gamma^{(i)}}(t)\bar{\mathbf{x}}(t) + \mathbf{v}_1^{(i)}(t), \quad t \geq 1$$

where

$$\mathcal{D}_1^{\gamma^{(i)}}(t) = \mathcal{T}_1 \text{diag} \left(\gamma^{(i)r}(t) \right) \mathcal{T}_n^{\text{H}}, \quad i = 1, \dots, m,$$

with

$$\mathcal{T}_1 = \frac{1}{2} \begin{bmatrix} 1 & \eta & \eta' & \eta'' \end{bmatrix} \otimes \mathbf{I}_n. \quad (8)$$

Then,

$$\Pi_1^{\gamma^{(i)}}(t) = E \left[\mathcal{D}_1^{\gamma^{(i)}}(t) \right] = \left[\Pi_1^{(i)}(t), \mathbf{0}_{n \times 3n} \right], \quad (9)$$

where $\Pi_1^{(i)}(t)$ is given in (5), and $\mathbf{0}_{n \times 3n}$ represents the $n \times 3n$ zero matrix.

- In the \mathbb{T}_2 -proper scenario. Now the processes $\bar{\mathbf{x}}(t)$, $\bar{\mathbf{u}}(t)$, $\bar{\mathbf{y}}^{(i)}(t)$, $\bar{\mathbf{v}}^{(i)}(t)$ and $\bar{\Phi}(t)$, are substituted by $\mathbf{x}_2(t) \triangleq [\mathbf{x}(t), \mathbf{x}^{\text{H}}(t)]^{\text{T}}$, $\mathbf{u}_2(t) \triangleq [\mathbf{u}(t), \mathbf{u}^{\text{H}}(t)]^{\text{T}}$, $\mathbf{z}_2^{(i)}(t) \triangleq [\mathbf{z}^{(i)}(t), \mathbf{z}^{(i)\text{H}}(t)]^{\text{T}}$, $\mathbf{v}_2^{(i)}(t) \triangleq [\mathbf{v}^{(i)}(t), \mathbf{v}^{(i)\text{H}}(t)]^{\text{T}}$ and $\Phi_2(t)$ (defined in (6)). The *pseudo* variance and cross-covariance matrices of the noises are denoted by $\mathbf{Q}_2(t)$, $\mathbf{R}_2^{(i)}(t)$ and $\mathbf{S}_2^{(i)}(t)$. The reduced observation equation is now expressed as

$$\mathbf{y}_2^{(i)}(t) = \mathcal{D}_2^{\gamma^{(i)}}(t)\bar{\mathbf{x}}(t) + \mathbf{v}_2^{(i)}(t), \quad t \geq 1$$

where

$$\mathcal{D}_2^{\gamma^{(i)}}(t) = \mathcal{T}_2 \text{diag} \left(\gamma^{(i)r}(t) \right) \mathcal{T}_n^{\text{H}}, \quad i = 1, \dots, m,$$

with

$$\mathcal{T}_2 = \frac{1}{2} \begin{bmatrix} 1 & \eta & \eta' & \eta'' \\ 1 & -\eta & \eta' & -\eta'' \end{bmatrix} \otimes \mathbf{I}_n, \quad (10)$$

and

$$\Pi_2^{\gamma^{(i)}}(t) = E \left[\mathcal{D}_2^{\gamma^{(i)}}(t) \right] = \left[\Pi_2^{(i)}(t), \mathbf{0}_{2n \times 2n} \right], \quad (11)$$

where $\Pi_2^{(i)}(t)$ is given in (7).

3 OPTIMAL PREDICTION ALGORITHM

In this section, the optimal one-stage prediction problem of the signal $\mathbf{x}(t)$ from all the observations provided by the m sensors is addressed, under \mathbb{T}_k -properness conditions. So, denoting by $\bar{\mathbf{y}}(t)$ the vector formed by the observations from all the sensors, that is, $\bar{\mathbf{y}}(t) = [\bar{\mathbf{y}}^{(1)\text{T}}(t), \dots, \bar{\mathbf{y}}^{(m)\text{T}}(t)]^{\text{T}}$, our aim is to obtain recursive formulas to obtain the optimal least-squares linear estimator of the signal $\mathbf{x}(t)$ from the observations until previous instant, $\{\bar{\mathbf{y}}(1), \dots, \bar{\mathbf{y}}(t-1)\}$. The observation equation is now expressed as follows

$$\bar{\mathbf{y}}(t) = \bar{\mathcal{D}}^{\bar{\gamma}}(t)\Lambda_n\bar{\mathbf{x}}(t) + \bar{\mathbf{v}}(t), \quad t \geq 1$$

where $\bar{\mathcal{D}}^{\bar{\gamma}}(t) = \Upsilon_n \text{diag} \left(\bar{\gamma}_j^{\text{T}}(t) \right) \Upsilon_n^{\text{H}}$, with $\Upsilon_n = \mathbf{I}_m \otimes \mathcal{T}_n$,

and $\bar{\gamma}_j^{\text{T}}(t) = [\gamma_j^{(1)r^{\text{T}}}(t), \dots, \gamma_j^{(m)r^{\text{T}}}(t)]^{\text{T}}$, $\Lambda_n = \mathbf{1}_m \otimes \mathbf{I}_{4n}$,

where $\mathbf{1}_m$ denotes the $m \times 1$ vector with all its elements 1, and $\bar{\mathbf{v}}(t) = [\bar{\mathbf{v}}^{(1)\text{T}}(t), \dots, \bar{\mathbf{v}}^{(m)\text{T}}(t)]^{\text{T}}$. The

pseudo variance and cross-covariance matrices of the additive noises are given by: $\bar{\mathbf{R}}(t) = E [\bar{\mathbf{v}}(t)\bar{\mathbf{v}}^{\text{H}}(t)] = \text{diag} \left(\bar{\mathbf{R}}^{(1)}(t), \dots, \bar{\mathbf{R}}^{(m)}(t) \right)$, $E [\bar{\mathbf{u}}(t)\bar{\mathbf{v}}^{\text{H}}(s)] = \bar{\mathbf{S}}(t)\delta_{ts}$,

with $\bar{\mathbf{S}}(t) = [\bar{\mathbf{S}}^{(1)}(t), \dots, \bar{\mathbf{S}}^{(m)}(t)]$.

However, under \mathbb{T}_k -properness conditions, for $k = 1, 2$, a reduction of the dimension in the state-space model is obtained; so, assuming this property, the observation equation is given as follows

$$\mathbf{y}_k(t) = \bar{\mathcal{D}}_k^{\bar{\gamma}}(t)\Lambda_n\bar{\mathbf{x}}(t) + \bar{\mathbf{v}}(t), \quad t \geq 1, \quad (12)$$

where $\bar{\mathcal{D}}_k^{\bar{\gamma}}(t) = \Upsilon_k \text{diag} \left(\bar{\gamma}_j^{\text{T}}(t) \right) \Upsilon_k^{\text{H}}$, with $\Upsilon_k = \mathbf{I}_m \otimes \mathcal{T}_k$, and \mathcal{T}_k for $k = 1, 2$ are given in (8) and (10), respectively. Moreover,

$$\begin{aligned}\bar{\Pi}_k^{\bar{\gamma}}(t) &= E \left[\bar{\mathcal{D}}_k^{\bar{\gamma}}(t) \right] \\ &= \text{diag} \left(\Pi_k^{\gamma^{(1)}}(t), \dots, \Pi_k^{\gamma^{(m)}}(t) \right),\end{aligned}$$

with $\Pi_k^{(i)}(t)$, for $i = 1, \dots, m$, given in (9) and (11) for $k = 1, 2$, respectively.

Next result proposes a recursive algorithm to obtain the optimal one-stage predictor under \mathbb{T}_k -properness conditions, denoted by $\hat{\mathbf{x}}^{\mathbb{T}_k}(t|t-1)$, as well as its mean squared error.

Theorem 1. Under \mathbb{T}_k -properness conditions, for $k = 1, 2$, in the model described by equations (2) and (12) and the hypotheses assumed, the optimal one-stage predictor, $\hat{\mathbf{x}}^{\mathbb{T}_k}(t|t-1)$, is obtained by extracting the first n components of $\hat{\mathbf{x}}_k(t|t-1)$, which is recursively calculated as follows

$$\hat{\mathbf{x}}_k(t|t-1) = \Phi_k(t-1)\hat{\mathbf{x}}_k(t-1|t-1) + \mathbf{H}_k(t-1)\boldsymbol{\varepsilon}_k(t-1), \quad t \geq 2,$$

where $\hat{\mathbf{x}}_k(t-1|t-1)$ satisfies this formula

$$\hat{\mathbf{x}}_k(t-1|t-1) = \hat{\mathbf{x}}_k(t-1|t-2) + \mathbf{L}_k(t-1)\boldsymbol{\varepsilon}_k(t-1), \quad t \geq 2,$$

with initial conditions $\hat{\mathbf{x}}_k(1|0) = \hat{\mathbf{x}}_k(0|0) = \mathbf{0}_{kn}$. The matrices $\mathbf{H}_k(t)$ and $\mathbf{L}_k(t)$ are calculated as: $\mathbf{H}_k(t) = \mathbf{S}_k(t)\boldsymbol{\Omega}_k^{-1}(t)$ and $\mathbf{L}_k(t) = \boldsymbol{\Theta}_k(t)\boldsymbol{\Omega}_k^{-1}(t)$, where $\mathbf{S}_k(t) = [\mathbf{S}_k^{(1)}(t), \dots, \mathbf{S}_k^{(m)}(t)]$, with $\mathbf{S}_k^{(i)}(t)$, for $i = 1, \dots, m$, defined in Section 2.2.

The innovations, $\boldsymbol{\varepsilon}_k(t)$, are obtained as follows

$$\boldsymbol{\varepsilon}_k(t) = \mathbf{y}_k(t) - \Pi_k(t)\Lambda_k\hat{\mathbf{x}}_k(t|t-1), \quad t \geq 1,$$

where $\Lambda_k = \mathbf{1}_m \otimes \mathbf{I}_{kn}$, and $\Pi_k(t) = \text{diag}(\Pi_k^{(1)}(t), \dots, \Pi_k^{(m)}(t))$, with $\Pi_k^{(i)}(t)$ for $k = 1, 2$, are given in (5) and (7), respectively.

The matrices $\boldsymbol{\Theta}_k(t)$ satisfy this relation

$$\begin{aligned} \boldsymbol{\Theta}_k(t) &= \mathbf{P}_k(t|t-1)\Lambda_k^T\Pi_k(t), \quad t \geq 2; \\ \boldsymbol{\Theta}_k(1) &= \mathbf{1}_m^T \otimes \mathbf{D}_k(1)\Pi_k(1), \end{aligned}$$

with

$$\begin{aligned} \mathbf{D}_k(1) &= [\mathbf{I}_{kn}, \mathbf{0}_{kn \times (4-k)n}] \left(\bar{\Phi}(0)\bar{\mathbf{P}}(0)\bar{\Phi}^H(0) + \bar{\mathbf{Q}}(0) \right) \\ &\quad \times [\mathbf{I}_{kn}, \mathbf{0}_{kn \times (4-k)n}]^T. \end{aligned}$$

The pseudo covariance matrix of the innovations, $\boldsymbol{\Omega}_k(t)$, is obtained from this expression

$$\begin{aligned} \boldsymbol{\Omega}_k(t) &= \Upsilon_k \left(\text{Cov}(\bar{\gamma}^r(t)) \circ (\Upsilon_n^H \Lambda_n \bar{\mathbf{D}}(t) \Lambda_n^T \Upsilon_n) \right) \Upsilon_k^H \\ &\quad + \Pi_k(t)\boldsymbol{\Xi}_k\mathbf{P}_k(t|t-1)\boldsymbol{\Xi}_k^T\Pi_k(t) \\ &\quad + \mathbf{R}_k(t), \quad t \geq 2, \\ \boldsymbol{\Omega}_k(1) &= \mathbf{I}_m \otimes \Pi_k(1)\mathbf{D}_k(1)\Pi_k(1) + \mathbf{R}_k(1), \end{aligned}$$

where $\bar{\mathbf{D}}(t)$ can be recursively calculated by this formula

$$\begin{aligned} \bar{\mathbf{D}}(t) &= \bar{\Phi}(t-1)\bar{\mathbf{D}}(t-1)\bar{\Phi}^H(t-1) + \bar{\mathbf{Q}}(t-1), \quad t \geq 1, \\ \bar{\mathbf{D}}(0) &= \bar{\mathbf{P}}_0. \end{aligned}$$

and $\mathbf{R}_k(t) = \text{diag}(\mathbf{R}_k^{(1)}(t), \dots, \mathbf{R}_k^{(m)}(t))$, with $\mathbf{R}_k^{(i)}(t)$, for $i = 1, \dots, m$, defined in Section 2.2.

Finally, the prediction error covariance matrices, $\mathbf{P}^{\mathbb{T}_k}(t|t-1)$, are calculated from $\mathbf{P}_k(t|t-1)$, which satisfy the following equation

$$\begin{aligned} \mathbf{P}_k(t|t-1) &= \Phi_k(t-1)\mathbf{P}_k(t-1|t-1)\Phi_k^H(t-1) \\ &\quad - \Phi_k(t-1)\boldsymbol{\Theta}_k(t-1)\mathbf{H}_k^H(t-1) \\ &\quad - \mathbf{H}_k(t-1)\boldsymbol{\Theta}_k^H(t-1)\Phi_k^H(t-1) \\ &\quad - \mathbf{H}_k(t-1)\boldsymbol{\Omega}_k(t-1)\mathbf{H}_k^H(t-1) \\ &\quad + \mathbf{Q}_k(t-1), \quad t \geq 1 \end{aligned}$$

where $\mathbf{P}_k(t-1|t-1)$ can be recursively obtained from this relation

$$\begin{aligned} \mathbf{P}_k(t-1|t-1) &= \mathbf{P}_k(t-1|t-2) \\ &\quad - \boldsymbol{\Theta}_k(t-1)\boldsymbol{\Omega}_k^{-1}(t-1) \\ &\quad \times \boldsymbol{\Theta}_k^H(t-1), \quad t \geq 1, \end{aligned}$$

with initial conditions

$$\mathbf{P}_k(0|0) = [\mathbf{I}_{kn}, \mathbf{0}_{kn \times (4-k)n}] \mathbf{P}_0 [\mathbf{I}_{kn}, \mathbf{0}_{kn \times (4-k)n}]^T,$$

and $\mathbf{P}_k(1|0) = \mathbf{D}_k(1)$.

4 NUMERICAL EXAMPLE

Our goal in this section is to illustrate the performance of the proposed estimator by considering the following tessarine state-space model with five sensors:

$$\begin{aligned} x(t+1) &= fx(t) + u(t), \quad t \geq 0, \\ y^{(i)}(t) &= \gamma_r^{(i)}(t)x_r(t) + \eta\gamma_\eta^{(i)}(t)x_\eta(t) + \eta'\gamma_{\eta'}^{(i)}(t)x_{\eta'}(t) \\ &\quad + \eta''\gamma_{\eta''}^{(i)}(t)x_{\eta''}(t) + v^{(i)}(t), \quad t \geq 1, \end{aligned}$$

for $i = 1, \dots, 5$, where $f = 0.9 + 0.3\eta + 0.1\eta' + 0.1\eta'' \in \mathbb{T}$, $\{\gamma_v^{(i)}(t); t \geq 1\}_{v=r,\eta,\eta',\eta''}$ are sequences of

Bernoulli random variables with parameters $p_v^{(i)}(t)$, and $u(t)$ and $v^{(i)}(t)$ are tessarine Gaussian noises.

Moreover, the real covariance matrix of $u(t)$ is given as follows

$$E[\mathbf{u}^r(t)\mathbf{u}^{r^T}(s)] = \begin{pmatrix} 0.9 & 0 & b & 0 \\ 0 & a & 0 & b \\ b & 0 & 0.9 & 0 \\ 0 & b & 0 & a \end{pmatrix} \delta_{ts}, \quad (13)$$

with $\mathbf{u}^r(t) = [u_r(t), u_\eta(t), u_{\eta'}(t), u_{\eta''}(t)]^T$.

The additive observation noises, $v^{(i)}(t)$, are defined as

$$v^{(i)}(t) = \alpha_i u(t) + w^{(i)}(t),$$

with $\alpha_1 = 0.5, \alpha_2 = 0.3, \alpha_3 = 0.4, \alpha_4 = 0.6, \alpha_5 = 0.2$, and $w^{(i)}(t)$ tesseract zero-mean white Gaussian noises with real covariance matrices

$$E \left[\mathbf{w}^{(i)r}(t) \mathbf{w}^{(i)r\top}(s) \right] = \text{diag}(\beta_i, \beta_i, \beta_i, \beta_i) \delta_{ts},$$

with $\mathbf{w}^{(i)r}(t) = [w_r^{(i)}(t), w_{\eta'}^{(i)}(t), w_{\eta''}^{(i)}(t), w_{\eta'''}^{(i)}(t)]^\top$ and $\beta_1 = 3, \beta_2 = 7, \beta_3 = 15, \beta_4 = 21, \beta_5 = 25$.

It is also assumed that the variance matrix of the real initial state is given as follows

$$E \left[\mathbf{x}^r(0) \mathbf{x}^{r\top}(0) \right] = \begin{pmatrix} c & 0 & d & 0 \\ 0 & 4 & 0 & d \\ d & 0 & c & 0 \\ 0 & d & 0 & 4 \end{pmatrix}, \quad (14)$$

with $\mathbf{x}^r(0) = [x_r(0), x_{\eta'}(0), x_{\eta''}(0), x_{\eta'''}(0)]^\top$.

Finally, the mutual independence hypothesis between the initial state and the multiplicative and additive noises is also considered.

The performance of the proposed estimator is analysed in both \mathbb{T}_1 and \mathbb{T}_2 -proper scenarios by taking different values of the Bernoulli parameters, assuming that these are constant in time, that is, for each $i = 1, \dots, 5, v = r, \eta', \eta'', p_v^{(i)}(t) = p_v^{(i)}$, for all t .

4.1 \mathbb{T}_1 -Proper Case

In order to guarantee the \mathbb{T}_1 -properness conditions, let us consider $a = 0.9, b = 0.3$ in (13), and $c = 4, d = -2.5$ in (14). Moreover, $p_v^{(i)} = p^{(i)}$, for $v = r, \eta', \eta''$. Under these assumptions, $x(t)$ and $y^{(i)}(t), i = 1, \dots, 5$ are jointly \mathbb{T}_1 -proper.

Firstly, in order to show the effectiveness of the proposed estimator in comparison with the one-stage predictor obtained at each sensor, the error variances are computed in Figure 1 for the following values of the Bernoulli parameters: Sensor 1, $p^{(1)} = 0.9$; Sensor 2, $p^{(2)} = 0.7$; Sensor 3, $p^{(3)} = 0.5$; Sensor 4, $p^{(4)} = 0.3$; Sensor 5, $p^{(5)} = 0.1$. It is observed that the performance of the proposed estimator, that uses the observations provided for all the sensors, is better than any of the estimators obtained from the observations of each sensor. Note that the probability that the observation at each sensor contains the signal decreases from Sensor 1 to 5, that is, at Sensor 1, it is more probable that the observation contains signal and noise, but the opposite happens at Sensor 5, it is more probable that the observation contains only noise. As it is observed, as this probability decreases, from Sensor 1 to 5, the error variances increase, and then the accuracy of the estimator is worse.

Now, in order to show the performance of the proposed estimator with regards to the Bernoulli probabilities, the error variances are computed for different

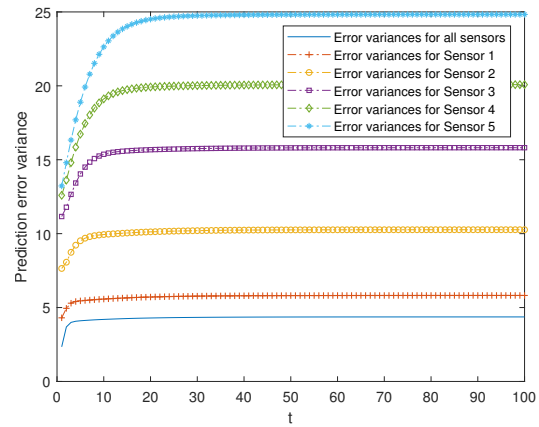


Figure 1: Prediction error variances for the proposed estimator and for the one obtained from the observations at Sensor i , for $i = 1, \dots, 5$.

values of them. Specifically, the same probability has been taken in all the sensors, decreasing from 0.9 to 0.1, that is, the following situations have been considered: $p^{(i)} = 0.9, \forall i; p^{(i)} = 0.7, \forall i; p^{(i)} = 0.5, \forall i; p^{(i)} = 0.3, \forall i$ and $p^{(i)} = 0.1, \forall i$. As before, it is observed that as the Bernoulli probabilities of all the sensors decrease, which means that it is more probable that the observations contain more noise and less signal, the error variances increase and hence, the estimations are worse.

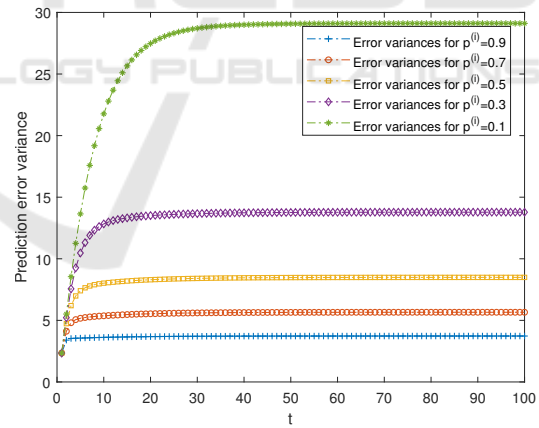


Figure 2: Prediction error variances for the proposed estimator taking the same probability in all the sensors.

4.2 \mathbb{T}_2 -Proper Case

Consider the values $a = 0.6, b = 0.3$ in (13), and $c = 3, d = -2.5$ in (14), and also, $p_r^{(i)} = p_{\eta'}^{(i)}$ and $p_{\eta''}^{(i)} = p_{\eta'''}^{(i)}$. So, $x(t)$ and $y^{(i)}(t), i = 1, \dots, 5$ are jointly \mathbb{T}_2 -proper.

Now, under \mathbb{T}_2 -properness conditions, analogous situations to Figures 1 and 2, have been illustrated

in Figures 3 and 4, respectively. For this purpose, in Figure 3, the prediction error variances for the proposed estimator which uses the observations of all the sensors, as well as for the estimator at each sensor, are shown by taking the following probability values: Sensor 1, $(p_r^{(1)}, p_{\eta'}^{(1)}) = (0.9, 0.8)$; Sensor 2, $(p_r^{(2)}, p_{\eta'}^{(2)}) = (0.7, 0.6)$; Sensor 3, $(p_r^{(3)}, p_{\eta'}^{(3)}) = (0.5, 0.4)$; Sensor 4, $(p_r^{(4)}, p_{\eta'}^{(4)}) = (0.3, 0.2)$; Sensor 5, $(p_r^{(5)}, p_{\eta'}^{(5)}) = (0.1, 0.05)$. And, in Figure 4, the prediction error variances for the proposed estimator have been displayed by considering the same probability in all the sensors at these situations: $(p_r^{(i)}, p_{\eta'}^{(i)}) = (0.9, 0.8), \forall i$; $(p_r^{(i)}, p_{\eta'}^{(i)}) = (0.7, 0.6), \forall i$; $(p_r^{(i)}, p_{\eta'}^{(i)}) = (0.5, 0.4), \forall i$; $(p_r^{(i)}, p_{\eta'}^{(i)}) = (0.3, 0.2), \forall i$; and $(p_r^{(i)}, p_{\eta'}^{(i)}) = (0.1, 0.05), \forall i$. Analogous considerations to that of Figures 1 and 2, in the \mathbb{T}_1 -proper case, are deduced.

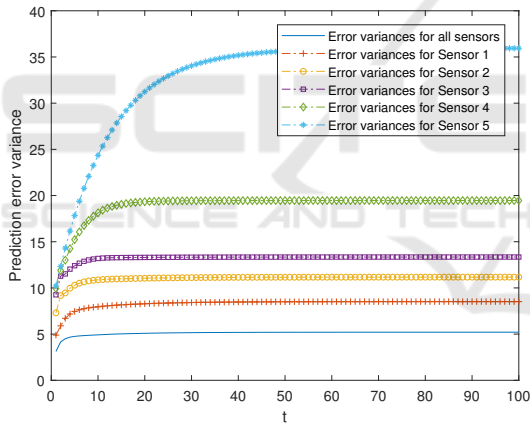


Figure 3: Prediction error variances for the proposed estimator and for the one obtained from the observations at Sensor i , for $i = 1, \dots, 5$.

5 CONCLUSIONS

Recently, the scientific community has shown an increasing interest in the use of hypercomplex algebras to model many experimental phenomena, as well as in assuming that the observations of the signal to be estimated are provided by multiple sensors. The first aim is due to the fact that the hypercomplex domains are more appropriate than the real field to describe a great amount of physical variables and also, under certain properness conditions, a reduction in the computational burden involved in the estimation al-

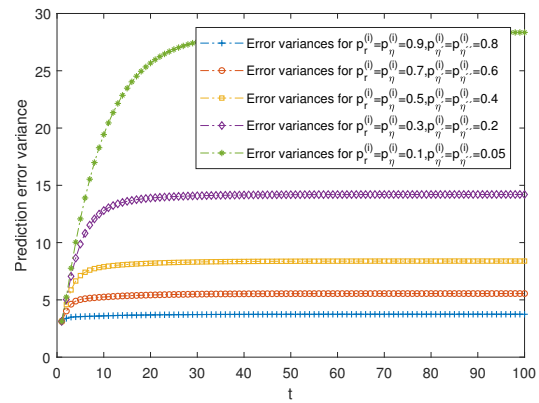


Figure 4: Prediction error variances for the proposed estimator taking the same probability in all the sensors.

gorithms is attained. The last goal is due to the fact that the use of multisensor observations yields better estimations.

The generalization of the signal processing results obtained in the real field to the hypercomplex domain is not immediate. Some of the main properties of the algebraic operations in the real field are not valid in the hypercomplex domains. Until now, most of the results obtained on hypercomplex signal estimation have been approached in the quaternion domain, since it has a Hilbert space structure. However, commutative hypercomplex algebras such as tessarines, provide a suitable structure to extend the main results in the real and complex field to this one. Although the tessarine domain is not a Hilbert space, a norm has been recently defined to guarantee the existence and uniqueness of the optimal least squares linear estimator (Navarro-Moreno et al., 2020). From this last result, the tessarine signal estimation problem is currently an important research object.

ACKNOWLEDGEMENTS

This work has been supported in part by I+D+i project with reference number 1256911, under ‘Programa Operativo FEDER Andalucía 2014-2020’, Junta de Andalucía, and Project EI-FQM2-2021 of ‘Plan de Apoyo a la Investigación 2021-2022’ of the University of Jaén.

REFERENCES

Abbasi-Kesbi, R. and Nikfarjam, A. (2018). A miniature sensor system for precise hand position monitoring. *IEEE Sensors Journal*, 18(6):2577–2584.
 Ahmad, Z., Hashim, S., Rokhani, F., Al-Haddad, S., Sali,

- A., and Takei, K. (2021). Quaternion model of higher-order rotating polarization wave modulation for high data rate m2m lpwan communication. *Sensors*, 21:383.
- Ajdaroski, M., Ashton-Miller, J., Baek, S., Shahshahani, P., and Esquivel, A. (2022). Testing a quaternion conversion method to determine human three-dimensional tibiofemoral angles during an in vitro simulated jump landing. *Journal of biomechanical engineering*, 144(4):041002.
- Augereau, B. and Carré, P. (2017). Hypercomplex polynomial wavelet-filter bank transform for color image. *Signal Processing*, 136:16–28.
- Bayro-Corrochano, E., Solis-Gamboa, S., Altamirano-Escobedo, G., Lechuga-Gutierrez, L., and Lisarraga-Rodríguez, J. (2021). Quaternion spiking and quaternion quantum neural networks: Theory and applications. *International Journal of Neural Systems*, 31(2):2050059.
- Celsi, M., Scardapane, S., and Comminiello, D. (2020). Quaternion neural networks for 3d sound source location in reverberant environments. In *MLSP'2020, IEEE international Workshop on Machine Learning for Signal Processing*, page 9231809.
- Fernández-Alcalá, R. M., Navarro-Moreno, J., Jiménez-López, J. D., and Ruiz-Molina, J. C. (2020). Semi-widely linear estimation algorithms of quaternion signals with missing observations and correlated noises. *Journal of the Franklin Institute*, 357:3075–3096.
- Fernández-Alcalá, R. M., Navarro-Moreno, J., and Ruiz-Molina, J. C. (2021). T-proper hypercomplex centralized fusion estimation for randomly multiple sensor delays systems with correlated noises. *Sensors*, 21(17):5729.
- Grakhova, E., Abdrakhmanova, G., Schmidt, S., Vinogradova, I., and Sultanov, A. (2019). The quadrature modulation of quaternion signals for capacity upgrade of high-speed fiber-optic wireless communication systems. In *SPIE - The Society for Optical Engineering*, page 11146.
- Jiménez-López, J. D., Fernández-Alcalá, R. M., Navarro-Moreno, J., and Ruiz-Molina, J. C. (2017). Widely linear estimation of quaternion signals with intermittent observations. *Signal Processing*, 136:92–101.
- Liang, J., Shen, B., Dong, H., and Lam, J. (2011). Robust distributed state estimation for sensor networks with multiple stochastic communication delays. *International Journal of Systems Science*, 42(9):1459–1471.
- Lin, H. and Sun, S. (2016). Distributed fusion estimator for multi-sensor asynchronous sampling systems with missing measurements. *IET Signal Processing*, 10(7):724–731.
- Linares-Pérez, J., Carazo, A. H., Caballero-Águila, R., and Jiménez-López, J. D. (2009). Least-squares linear filtering using observations coming from multiple sensors with one- or two-step random delay. *Signal Processing*, 89(10):2045–2052.
- Liu, W.-Q., Wang, X.-M., and Deng, Z.-L. (2017). Robust centralized and weighted measurement fusion kalman estimators for uncertain multisensor systems with linearly correlated white noises. *Information Fusion*, 35:11–25.
- Ma, J. and Sun, S. (2013). Centralized fusion estimators for multisensor systems with random sensor delays, multiple packet dropouts and uncertain observations. *IEEE Sensors Journal*, 13:1228–1235.
- Navarro-Moreno, J., Fernández-Alcalá, R. M., Jiménez-López, J. D., and Ruiz-Molina, J. C. (2019). Widely linear estimation for multisensor quaternion systems with mixed uncertainties in the observations. *Journal of the Franklin Institute*, 356:3115–3138.
- Navarro-Moreno, J., Fernández-Alcalá, R. M., Jiménez-López, J. D., and Ruiz-Molina, J. C. (2020). Tessarine signal processing under the T-properness condition. *Journal of the Franklin Institute*, 357(14):10099–10125.
- Navarro-Moreno, J. and Ruiz-Molina, J. C. (2021). Wide-sense markov signals on the tessarine domain. a study under properness conditions. *Signal Processing*, 183:108022.
- Ortolani, F., Comminiello, D., and Uncini, A. (2016). The widely linear block quaternion least mean square algorithm for fast computation in 3d audio systems. In *MLSP'2016, IEEE international Workshop on Machine Learning for Signal Processing*, page 7738842.
- Qu, Y. and Yi, W. (2022). Three-dimensional obstacle avoidance strategy for fixed-wing uavs based on quaternion method. *Applied Sciences*, 12(3):955.
- Wei, W., Yu, J., Wang, L., Hu, C., and Jiang, H. (2022). Fixed/preassigned-time synchronization of quaternion-valued neural networks via pure power-law control. *Neural Networks*, 146:341–349.
- Yang, L., Miao, J., and Kou, K. (2022). Quaternion-based color image completion via logarithmic approximation. *Information Sciences*, 588:82–105.
- Zhang, J., Gao, S., Li, G., Xia, J., Qi, X., and Gao, B. (2021). Distributed recursive filtering for multi-sensor networked systems with multi-step sensor delays, missing measurements and correlated noise. *Signal Processing*, 181:107868.
- Zheng, J., Wang, H., and Pei, B. (2020). Uav attitude measurement in the presence of wind disturbance. *Signal, Image and Video Processing*, 14(8):1517–1524.